

# Influence of a charge region on the operation of InGaAs/InAlAs/InP avalanche photodiodes

JAROSŁAW JUREŃCZYK<sup>1,2\*</sup>, DARIUSZ ŻAK<sup>2</sup>, JANUSZ KANIEWSKI<sup>2</sup>

<sup>1</sup>Wrocław University of Technology, Faculty of Microsystem Electronics and Photonics,  
ul. Janiszewskiego 11/17, 50-372 Wrocław, Poland

<sup>2</sup>Institute of Electron Technology, al. Lotników 32/46, 02-668 Warszawa, Poland

\*Corresponding author: jjurenczyk@ite.waw.pl

Avalanche photodiodes (APDs) operating at 1.55 μm wavelength are used in many different applications. Therefore, specialized devices with modified electrical characteristics are often strongly needed. In order to design and produce such structures, advanced modeling techniques and computer aided design (CAD) software are utilized. In the paper, modeling results of avalanche photodiodes with separated regions of absorption, grading, charge and multiplication (SAGCM) are presented. Simulations of diode structures were performed using APSYS software developed by Crosslight. Extensive calculations allowed for the detailed analysis of individual regions of the device and the determination of their influence on diode characteristics. Simulations showed a pronounced influence of the charge region on characteristics and performance of the device. Changes of the doping level of this layer exhibited strong modification in the band-to-band tunnelling effect. Simultaneously it influenced the characteristics related to the Zener effect and carrier transport.

Keywords: avalanche photodiode, device modeling, InGaAs.

## 1. Introduction

Avalanche photodiodes (APDs) are significant photonic devices these days [1]. APDs provide increased sensitivity by internal gain. Simultaneously, the avalanche gain by hole-electron pair generation at high electric fields is inevitably subject to multiplication noise, restricting the device performance and maximum gain [2]. At first fiber optic telecommunication stimulated research and development of these devices. Presently, high-speed and high-sensitivity APDs are widely used in long-haul, high-bit rate telecommunication systems. Generally, comparing conventional *p-i-n* and APD based receivers, those working with APDs achieve better sensitivities, about 5–10 dB greater [3].

Recently, critical sensing and imaging applications, such as astronomical observations, space-related spectroscopy, confocal microscopy, optical range finding

and others, stimulated development of modified APD structures operating at 1.55 μm wavelength. For these devices speed is not critical. Instead, very low dark current densities and low multiplication noise are the main requirements.

Device designing required extended computer aided numerical simulations. In the calculations many physical models, phenomena and interactions between them have to be taken into account. Therefore, good effect understanding, properly chosen, well described mathematical models and modern software are needed to simulate device operation precisely. In the paper, simulation techniques based on the drift-diffusion model implemented in Crosslight APSYS software have been performed on conventional APDs with separated regions of absorption and multiplication. Various APDs structures with charge region, such as differing in doping level and thickness of layer, have been considered. Simulations show significant influence of a charge region on static dark currents as well as on basic dynamic electrical characteristics and carrier transport through different regions of the device.

## 2. APSYS modeling details

The Crosslight APSYS is a software program which allows for modeling semiconductor devices. In the program, the method of finite elements analysis is implemented to the solver. APSYS solves three basic equations: Poisson equation (1), and current continuity equations for electrons (2) and holes (3) [4]. Many physical models are available in Crosslight software. Basic models used in simulations are as follows: model of Shockley–Read–Hall and Auger recombination, model of incomplete ionization, carrier statistic and carrier mobility model. Several carrier mobility assumptions can be considered, *i.e.*, constant mobility, simplified field dependent mobility, field dependent mobility, III–V materials mobility and Poole–Frenkel mobility. Additionally, in devices operating under a reversed bias, the tunneling model corresponding with the Zener effect is important and taken into account.

$$-\nabla \left( \frac{\epsilon_0 \epsilon_{dc}}{q} \nabla V \right) = -n + p + N_D(1 - f_D) - N_A f_A + \sum_j N_{tj}(\delta_j - f_{tj}) \quad (1)$$

$$\nabla J_n - \sum_j R_n^{tj} - R_{sp} - R_{st} - R_{au} + G_{opt}(t) = \frac{\partial p}{\partial t} + N_D \frac{\partial f_D}{\partial t} \quad (2)$$

$$\nabla J_p + \sum_j R_p^{tj} + R_{sp} + R_{st} + R_{au} - G_{opt}(t) = -\frac{\partial p}{\partial t} + N_A \frac{\partial f_A}{\partial t} \quad (3)$$

where:  $V$  – the electrical potential,  $\epsilon_{dc}$  – the relative DC dielectric constant,  $n$  – electrons concentration,  $p$  – holes concentration,  $N_D$  – shallow donor density,  $N_A$  – shallow acceptors density,  $f_D$  – occupancy of the donor level,  $f_A$  – occupancy of the acceptor level,  $J_n$  and  $J_p$  – electron and hole current, respectively,  $R_n^{tj}$  and  $R_p^{tj}$  – electron and

hole recombination rates per unit volume through the  $j$ -th deep level, respectively,  $G_{\text{opt}}$  – optical generation rate,  $R_{\text{sp}}$ ,  $R_{\text{st}}$ , and  $R_{\text{au}}$  – spontaneous recombination rate, stimulated recombination rate and the Auger recombination rate per unit volume, respectively.

It is generally accepted that impact ionization can be described by Baraff's model and Chynoweth's formula. Both of them are implemented into APSYS solver.

The following equation shows generalized formula for electron and hole impact ionization coefficients,  $\alpha$  and  $\beta$ , respectively:

$$\alpha, \beta = A_C \exp \left[ - \left( \frac{F_c}{F} \right)^{k_n} \right] \quad (4)$$

where  $A_C$ ,  $F_c$  and  $k_n$  are empirical parameters, which are different for electrons and holes.

Generation rate  $G$  of the impact ionization equation:

$$G = \frac{\alpha J_n + \beta J_p}{q} \quad (5)$$

Tunneling currents in the reverse biased  $p-n$  junction are calculated using the following formula:

$$G_{\text{Zener}}(F) = \frac{dJ}{qdx} = \frac{gFm^*}{2\pi^2\hbar^3} P_0 \underline{E} \quad (6)$$

and parameters in that formula are given by:

$$P_0 = \exp \left[ \frac{\pi(m^*)^{1/2} E_g^{3/2}}{2(2)^{1/2} qF\hbar} \right] = \exp \left( -\frac{E_g}{4\underline{E}} \right) \quad (7)$$

$$\underline{E} = \frac{(2)^{1/2} qF\hbar}{2\pi(m^*)^{1/2} E_g^{1/2}} \quad (8)$$

where:  $G_{\text{Zener}}$  – Zener generation rate,  $F$  – electric field,  $m^*$  – effective tunneling mass,  $\hbar$  – reduced Planck constant,  $E_g$  – band gap of semiconductor,  $q$  – elementary charge,  $dJ/dx$  – tunneling current density flow,  $P_0$  – tunneling probability with a zero perpendicular momentum in  $x$  direction.

### 3. Structure of a simulated avalanche photodiode

A design of APD focuses on the optimization of three basic features of the device. Good quantum efficiency is reached when the absorber layer is relatively thick. On the other hand, when the absorbing space is large, a decrease in bandwidth is observed

Table 1. Schematic layer structure of the InGaAs/InAlAs/InP APD.

Cap	In <sub>0.53</sub> Ga <sub>0.47</sub> As	<i>p</i>	1.0×10 <sup>19</sup> cm <sup>-3</sup>	30 nm
Barrier	In <sub>0.52</sub> Al <sub>0.48</sub> As	<i>p</i>	1.0×10 <sup>19</sup> cm <sup>-3</sup>	200 nm
	In <sub>0.53</sub> Ga <sub>0.47</sub> As	<i>p</i>	2.5×10 <sup>18</sup> cm <sup>-3</sup>	150 nm
Absorber	In <sub>0.53</sub> Ga <sub>0.47</sub> As	<i>p</i>	1.0×10 <sup>18</sup> cm <sup>-3</sup>	150 nm
	In <sub>0.53</sub> Ga <sub>0.47</sub> As	<i>p</i>	4.0×10 <sup>17</sup> cm <sup>-3</sup>	150 nm
Grading	InGaAlAs		undoped	50 nm
Spacer	In <sub>0.52</sub> Al <sub>0.48</sub> As		undoped	100 nm
Charge	In <sub>0.52</sub> Al <sub>0.48</sub> As	<i>p</i>	4.0×10 <sup>17</sup> cm <sup>-3</sup>	90 nm
Multiplication	In <sub>0.52</sub> Al <sub>0.48</sub> As		undoped	150 nm
Buffer	In <sub>0.52</sub> Al <sub>0.48</sub> As	<i>n</i>	5.0×10 <sup>18</sup> cm <sup>-3</sup>	800 nm
Substrate	InP	<i>n</i>	SI	—

because much more carriers are generated and they need more time to achieve high field region. Dark current increases when doping in the absorber is at high level and the layer is located within depletion region. To minimize dark current and increase efficiency of avalanche photodiode, individual regions of this device are separated. Such segregation is asserted in SAGCM APD where regions of absorption, grading, charge, multiplication are separated [5, 6]. It is important to achieve high-sensitivities with minimal noise currents. In order to obtain an undepleted absorber, relatively thin absorption region and thin multiplication layer separated by spacer and charge regions were considered. Simulations have been performed for different thickness and doping level of charge region. Doping level of the layer has been changed in the range from 2×10<sup>16</sup> to 1×10<sup>18</sup> cm<sup>-3</sup> and thickness of the layer has been modified from 60 to 120 nm with 10 nm step. Scheme of the structure considered is presented in Tab. 1. All layers are lattice matched to semi-insulating InP substrate.

## 4. Results and discussion

In the simulations, various APD characteristics have been obtained. Calculated band diagram of the considered structure is presented in Fig. 1. The complete diagram shows shapes of the valence and conduction band as well as Fermi level position across the structure. All layers forming the device are clearly recognized. Additionally, positions of the regions are marked and labeled. This type of band diagram across the structure allows for verification correctness of the device design.

Further simulations have been performed for the structure under illumination and reverse bias. Light source operating at the wavelength equal to 1.55 μm and the power equal to 5 W/cm<sup>2</sup> was declared in an input solving file. Figure 2 presents current voltage (*I*–*V*) characteristics of dark and photocurrents. One can notice that dark

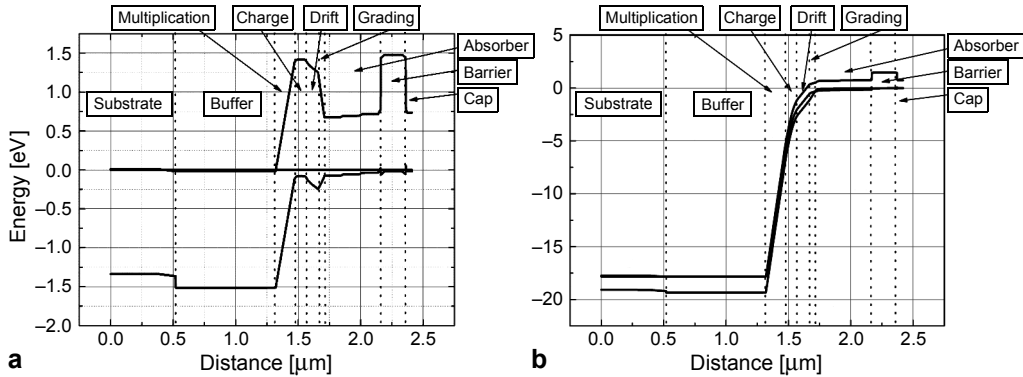


Fig. 1. Band diagram and regions across the device: at equilibrium (a), under polarization (b).

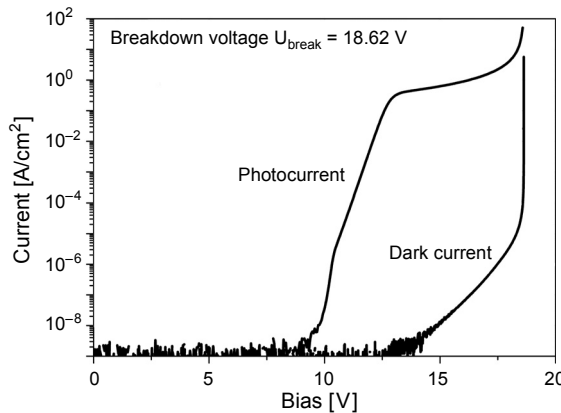


Fig. 2. Dark and photocurrent  $I$ - $V$  characteristic.

current is lower than  $1 \times 10^{-9}$  cm<sup>-2</sup> in the range of bias voltage below 13 V and it is correlated with the Zener tunneling effect. Avalanche breakdown in this structure is observed at higher voltage, *i.e.*, 18.62 V.

A family of electron current densities across the structure for different gains and magnitude of electric field for the gain equal to 100 is presented in Fig. 3. The analysis of the electron current flow clearly reveals the position of the multiplication region within the structure. Simultaneously, changes of electric field allow for localization of charge region. Phenomena of avalanche breakdown of the device depend strongly on doping level of charge layer. For lower doping levels lower voltage of avalanche breakdown is observed. Therefore, multiplication region should be intentionally undoped in order to obtain stronger impact ionization effect. Additionally, density of multiplied electron current depends on layer thickness. In thicker layer stronger gain can be reached. However, it is associated with higher multiplication noise.

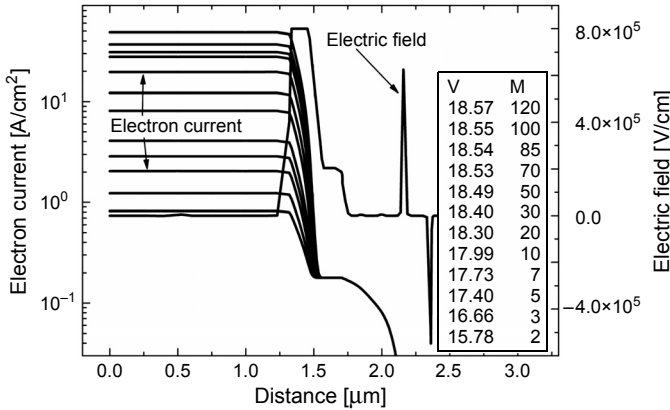


Fig. 3. Electron current and electric field across APD.

In simulated structures, the absorbing layer is separated from the internal field and depletion region to minimize dark current. The separation of the absorber is reached by a proper doping profile of the region and applying barrier and drift layers in the structure. The barrier layer blocks minority carriers originated from contact regions. Simultaneously, the undoped drift region widens the distance between the charge region and absorber. Step doping of the absorbing layer forms an extra electric field to aid carrier transport across the absorbing layer.

Surprisingly, the doping level of the charge layer is one of the most important parameters of the structure. The electric field is localized entirely between this layer and a buffer layer until avalanche breakdown is achieved. This region is very sensitive to doping changes and it creates significant differences in device characteristics.

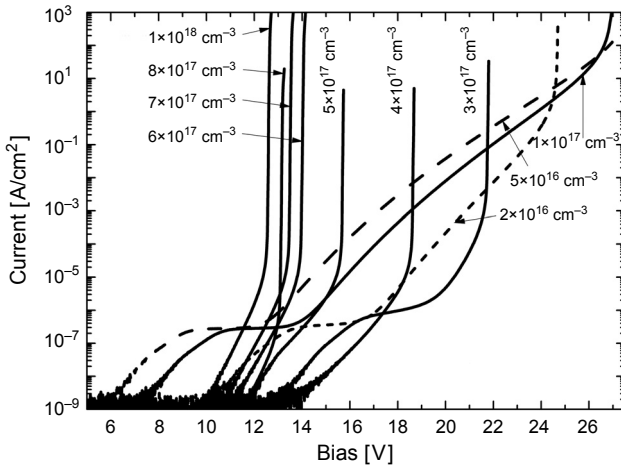


Fig. 4. Dark  $I$ - $V$  characteristics for different doping levels in charge region.

Figure 4 shows changes of breakdown voltage and dark current characteristics as a consequence of various doping levels of the charge region. Thickness of the layer is assumed to be 90 nm.

The doping level of the charge layer affects electric field across the structure. Field distribution causes difference in band bending in the band diagram. When the doping level is low, drift and grading regions are more deflected under the influence of local field. In the strong field, carriers (especially electrons) because of their effective mass, can exhibit band-to-band tunneling due to the Zener mechanism. For low doping levels, different breakdown effects are visible. In typical characteristics, at first breakdown related to the Zener effect is observed, next Zener and avalanche phenomena are visible and finally solely avalanche breakdown for the highest bias is observable.

Stronger doping of the charge layer causes screening drift region by the field generated by ionized acceptors. Then higher electric field is localized between the buffer and charge regions. At strong fields, the avalanche effect appears at lower voltages.

Thickness of the charge region significantly influences  $I$ - $V$  characteristics as well. Figure 5 presents current–voltage characteristics of photodiodes without illumination. In these structures, charge layer thickness changes from 60 to 120 nm. In all calculations the doping level equal to  $4 \times 10^{17} \text{ cm}^{-3}$  was assumed. Changes of breakdown voltage values and shapes of  $I$ - $V$  curves are strongly correlated with the field induced by dopant ions. Generally, a thicker layer triggered avalanche breakdown at lower voltage. On the other hand, a thinner charge layer allows electric field to deflect bands in a drift layer and therefore the Zener tunneling can be observed.

For doping levels, lower than  $4 \times 10^{17} \text{ cm}^{-3}$  increase of dark current occurs and considerable losses of gain are observed. When the doping level of the charge layer is higher than  $4 \times 10^{17} \text{ cm}^{-3}$ , barrier potential does not disappear when a photodiode is biased. The effect is important when the structure is illuminated. This barrier prevents

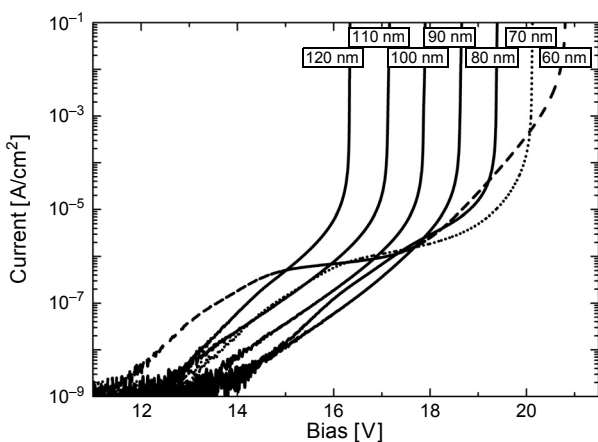


Fig. 5. Dark  $I$ - $V$  characteristics for different thicknesses of charge region.

the generated electrons from flowing and multiplying. Proper operation of the device at such conditions is not possible. For various thicknesses of the charge layer, the situation is similar.

## 5. Summary

Based on the advanced drift and diffusion model with the Crosslight APSYS, the InGaAs/InAlAs avalanche photodiodes have been simulated. The InGaAs/InAlAs/InP photodiodes with an undepleted *p*-type InGaAs absorber and a thin InAlAs multiplication layer are a system for 1.55  $\mu\text{m}$  wavelength detection. Simulated structures exhibit very low dark current, below  $1 \times 10^{-9} \text{ A/cm}^2$  and breakdown voltage at 18.62 V. These devices can be used in critical sensing and imaging applications.

*Acknowledgements* – This work was partially supported by The National Centre for Research and Development, Poland under project No. N R02 0025 06.

## References

- [1] CAMPBELL J.C., *Recent advances in telecommunications avalanche photodiodes*, Journal of Lightwave Technology **25**(1), 2007, pp. 109–121.
- [2] MCINTYRE R.J., *Multiplication noise in uniform avalanche diodes*, IEEE Transactions on Electron Devices **13**(1), 1966, pp. 164–168.
- [3] KANIEWSKI J., MUSZALSKI J., PIOTROWSKI J., *Advanced InGaAs/InAlAs/InP avalanche photodiodes for high-speed detection of 1.55  $\mu\text{m}$  infrared radiation*, Proceedings of SPIE **7082**, 2008, article 70820F.
- [4] XIAO Y.G., LI Z.Q., SIMON LI Z.M., *Dynamic drift-diffusion simulation of InP/InGaAs SAGCM APD*, Physica Status Solidi (c) **4**(5), 2007, pp. 1641–1645.
- [5] NING LI, RUBIN SIDHU, XIAOWEI LI, FENG MA, XIAOGUANG ZHENG, SHULING WANG, KARVE G., DEMIGUEL S., HOLMES A.L., CAMPBELL J.C., *InGaAs/InAlAs avalanche photodiode with undepleted absorber*, Applied Physics Letters **82**(13), 2003, pp. 2175–2177.
- [6] PARKS J.W., SMITH A.W., BRENNAN K.F., TAROF L.E., *Theoretical study of device sensitivity and gain saturation of separate absorption, grading, charge, and multiplication InP/InGaAs avalanche photodiodes*, IEEE Transactions on Electron Devices **43**(12), 1996, pp. 2113–2121.

*Received May 25, 2012  
in revised form August 22, 2012*